THE ASTROPHYSICAL JOURNAL, 420:439–444, 1994 January 10

MEASUREMENT OF THE COSMIC MICROWAVE BACKGROUND SPECTRUM BY THE *COBE*[1] FIRAS INSTRUMENT

J. C. MATHER,[2] E. S. CHENG,[2] D. A. COTTINGHAM,[3] R. E. EPLEE, JR.,[4] D. J. FIXSEN,[5] T. HEWAGAMA,[6] R. B. ISAACMAN,[4] K. A. JENSEN,[6] S. S. MEYER,[7] P. D. NOERDLINGER,[5] S. M. READ,[6] L. P. ROSEN,[6] R. A. SHAFER,[2] E. L. WRIGHT,[8] C. L. BENNETT,[2] N. W. BOGGESS,[2] M. G. HAUSER,[2] T. KELSALL,[2] S. H. MOSELEY, JR.,[2] R. F. SILVERBERG,[2] G. F. SMOOT,[9] R. WEISS,[7] AND D. T. WILKINSON[10]

Received 1993 February 5; accepted 1993 July 21

ABSTRACT

The cosmic microwave background radiation (CMBR) has a blackbody spectrum within 3.4×10^{-8} ergs cm^{-2} s^{-1} sr^{-1} cm over the frequency range from 2 to 20 cm^{-1} (5–0.5 mm). These measurements, derived from the FIRAS instrument on the *COBE* satellite, imply stringent limits on energy release in the early universe after $t \sim 1$ year and redshift $z \sim 3 \times 10^6$. The deviations are less than 0.03% of the peak brightness, with an rms value of 0.01%, and the dimensionless cosmological distortion parameters are limited to $|y| < 2.5 \times 10^{-5}$ and $|\mu| < 3.3 \times 10^{-4}$ (95% confidence level). The temperature of the CMBR is 2.726 ± 0.010 K (95% confidence level systematic).

Subject headings: cosmic microwave background — cosmology: observations — early universe

1. INTRODUCTION

1.1. *Background*

The FIRAS (Far-Infrared Absolute Spectrophotometer) instrument aboard the *COBE* (*Cosmic Background Explorer*) satellite (Boggess et al. 1992, and references therein; Bennett et al. 1993) was designed to measure the spectrum of the cosmic microwave background radiation (CMBR). The spectrum would have a blackbody form if the simple hot big bang model is a correct description of the early universe, but could be distorted from that form by energy release after a redshift $z \sim 3 \times 10^6$ (Peebles 1971; Sunyaev & Zel'dovich 1980). The CMBR was the dominant energy field at times after the annihilation of positrons and the decoupling of neutrinos until $z \sim 3 \times 10^4$, and the number of photons exceeds the number of baryons by a factor of the order of 10^9, so excellent sensitivity is required to detect even large radiant energy releases, as shown below in detail. Such releases might arise from decay of unstable particles, dissipation of cosmic turbulence and gravitational waves, breakdown of cosmic strings, and other more exotic transformations.

The CMBR was first observed by Penzias & Wilson (1965) and interpreted by Dicke et al. (1965). Early measurements were reviewed by Thaddeus (1972) and by Weiss (1980), and more recent measurements have been reviewed by Kogut (1993). Only weeks after the *COBE* was launched, the COBRA rocket experiment of Gush, Halpern, & Wishnow (1990) confirmed the results just reported by the FIRAS team (Mather et al. 1990). The CMBR temperature reported by the COBRA group was 2.736 ± 0.017 K, very close to the FIRAS result of 2.735 ± 0.060 K.

Preliminary spectrum distortion limits from the FIRAS were presented by Mather et al. (1990). These were based on 9 minutes of high Galactic latitude data taken early in the mission, and reduced with the first in-orbit calibration data. There was no deviation in the CMBR from an ideal blackbody spectrum by more than 1% of its peak brightness ($\Delta I_\nu < 1.2 \times 10^{-6}$ ergs cm^{-2} s^{-1} sr^{-1} cm) in the frequency range from 2 to 20 cm^{-1}. (Note: to convert these intensity units, which use a frequency unit of cm^{-1}, to SI values, 1 MJy $sr^{-1} = 2.9979 \times 10^{-7}$ ergs cm^{-2} s^{-1} sr^{-1} cm.) A later determination of the CMBR spectrum used over 1 hr of data taken near the direction which we have called Baade's Hole, now more commonly called Lockman's Hole (l, b) = (143°, 53°), which has a particularly small amount of contamination from Galactic dust emission. Refinements in the calibration ruled out any deviation from a blackbody by more than 0.25% (Shafer et al. 1992; Cheng 1992). The measured deviations were consistent with the expected amount and characteristic spectrum of Galactic dust. The initial FIRAS determination of the mean Galactic spectrum, as well as a number of atomic and molecular line intensities, were given by Wright et al. (1991). A map of the total far-IR flux was given, and luminosities for the lines and dust integrated over the entire Galaxy were obtained. Additional discussion of modeling the Galactic continuum emission using both the FIRAS and *COBE* DMR (Diffuse Microwave Radiometers) data is in Bennett et al. (1992).

1.2. *Current Results*

This paper is one of four describing the new results from the FIRAS, based on an improved understanding of the performance of the instrument in flight and the use of a larger fraction of the data than in previous papers. Here we report a

[1] The National Aeronautics and Space Administration/Goddard Space Flight Center (NASA/GSFC) is responsible for the design, development, and operation of the *Cosmic Background Explorer* (*COBE*). Scientific guidance is provided by the *COBE* Science Working Group. GSFC is also responsible for the development of the analysis software and for the production of the mission data sets.

[2] NASA Goddard Space Flight Center, Code 685, Greenbelt, MD 20771.
[3] Universities Space Research Association, Code 685.3, NASA/GSFC, Greenbelt, MD 20771.
[4] General Sciences Corporation, Code 685.3, NASA/GSFC, Greenbelt, MD 20771.
[5] Applied Research Corporation, Code 685.3, NASA/GSFC, Greenbelt, MD 20771.
[6] Hughes-STX, Code 685.9, NASA/GSFC, Greenbelt, MD 20771.
[7] MIT Department of Physics, Room 20F-001, Cambridge, MA 02139.
[8] UCLA Astronomy Department, Los Angeles, CA 90024-1562.
[9] LBL & SSL, Bldg 50-351, University of California, Berkeley, CA 94720.
[10] Princeton University Department of Physics, Princeton, NJ 08540.

new measurement of the CMBR spectrum and more stringent limits on distortions from a pure blackbody spectrum.

Fixsen et al. (1994b) describe the calibration procedures and the sources and treatment of systematic errors in the measurements. Fixsen et al. (1994a) determine the dipole spectrum from 2 to 20 cm^{-1}; it is the derivative of a blackbody spectrum, as anticipated, with a color temperature of 2.714 ± 0.022 K (95% CL [confidence level]). They find that the dipole is in the same direction as found by other methods and has an amplitude of 3.343 ± 0.016 mK (95% CL). The spectrum fits the prediction with an rms deviation of 6×10^{-9} ergs cm^{-2} s^{-1} sr^{-1} cm, only 0.005% of the peak intensity of the CMBR. The final paper of the series, Wright et al. (1994), compares these new results to previous measurements and interprets the spectrum deviation limits.

The instrument was calibrated using the method described in Fixsen et al. (1994b). The calibration was applied to the sky data, producing spectra from 2 to 20 cm^{-1}. Only sky data taken during the last 6 weeks of FIRAS operations were selected to derive the CMBR spectrum, since the instrument operation was stable and the calibrations were most frequent during that time. The CMBR spectrum was estimated from this data set after the Galactic emission and dipole spectrum had been removed. The spectral model of the Galactic emission and the dipole spectrum were derived from 10 months of data. Finally, the mean CMBR spectrum was analyzed to determine limits on the cosmic y and μ parameters.

2. INSTRUMENT DESIGN, OPERATION, AND DATA PROCESSING

The FIRAS instrument is a scanning polarizing Michelson interferometer, covering the wavelength range from 105 μm to 1 cm (Mather et al. 1990; Fixsen et al. 1994b). It has many special features to enable a comparison of the CMBR spectrum to a blackbody with a precision of the order of 0.01%. These include continuous differential comparison of the sky or an external blackbody calibrator to an internal reference calibrator adjusted to null the signal. The FIRAS optics are symmetrical, with two input and two output ports operated differentially. One input port receives emission from the sky, defined by a horn-shaped, nonimaging concentrator with a 7° beam width. During calibration the sky aperture is completely filled by an external blackbody with an emissivity greater than 0.9999, as known from ray trace calculations and microwave reflectance measurements. The external calibrator is isothermal to better than 1 mK according to calculations. The other input port receives emission from an internal reference calibrator with an associated concentrator. Each of the two output beams (arbitrarily labeled "left" and "right") is split by a dichroic filter into low- and high-frequency beams, separated at 20 cm^{-1}. Thus there are a total of four silicon composite bolometer detectors operated simultaneously.

The two calibrators and the two associated concentrators are temperature-controlled from 2 to 25 K. Redundant thermometers measure the temperatures of these four temperature controlled elements as well as other infrared emitters such as the moving mirrors, the mechanical structure, and the detector housings. When observing the sky the spectrometer is operated with its output nearly nulled, with the internal reference calibrator adjusted to match the sky temperature. This reduces sensitivity to gain errors and calibration drifts.

The path difference x between the two arms of the interferometer is varied by scanning a set of mirrors at a constant velocity. This motion produces a modulated power $P(x)$ at the output ports. $P(x)$ is approximately the cosine transform of the net power, i.e.,

$$P(x) \approx \tfrac{1}{2} \int_0^\infty dv \sum_{\text{inputs}} E_i(v) S_i(v) \cos(2\pi v x) . \quad (1)$$

Here E_i and S_i are the effective instrument *étendue* and the spectral intensity of each emitting input, and v is the frequency in cm^{-1}. The principal inputs are the sky (or external calibrator) and the internal calibrator, which are 180° out of phase. Each of the outputs of the interferometer also receives emission from other components of the instrument.

The mirrors can be scanned at one of two velocities ("slow" and "fast"), and over one of two lengths ("short" and "long"). This paper is restricted to data taken in one mirror scan mode, "short slow," which was used for about half the mission. We also use only the data taken by the "left low" bolometer, which had the best overall sensitivity in the 2–20 cm^{-1} interval. Further analysis of all the sky and calibration data from all detectors and scan modes may improve on the results given here, provided that systematic error and galactic modeling limits can also be improved. The stroke length determines the separation of 0.57 cm^{-1} between the 34 significant elements of the spectrum in this range. Apodization later smooths this resolution to 0.7 cm^{-1}.

On the ground, the interferograms are sorted into groups depending on instrument configuration and (for sky data) on the line of sight, so that all the interferograms in the group are nearly the same. The groups of interferograms are averaged and then converted to spectra by apodization and Fourier transformation. The spectra are corrected by dividing by the known analog and digital signal transfer functions of the amplifiers and microprocessors. Up to the production of raw spectra, sky data and calibration data are treated the same.

3. CALIBRATION

The calibration of the FIRAS is discussed in detail in Fixsen et al. (1994b). The model is derived from least-squares fits to data taken with the external calibrator in the aperture and with a wide variety of source temperatures. The residuals are of the order of 1% of the modulated signal levels. Several kinds of instrument errors were detected and included in the model. The calibration model was derived from all the calibration data except those taken in the first 2 months of the mission, when the instrument was not as stable.

The offset of the photometric system was determined from long observations of the external calibrator while it was adjusted to match the temperature of the sky. The observation time devoted to this part of the calibration limits the sensitivity of the measurement reported here. The data taken for this purpose were obtained in the last 6 weeks of the mission. There were 16,517 interferograms representing 10.1 days of integration included in the offset calculations. We calibrate them with the same model used for the sky data. The offset spectrum $c(v)$ is the weighted average of the residuals of the calibrated external calibrator spectra from best-fit blackbody spectra.

4. THE FIRAS TEMPERATURE SCALE

The first FIRAS results given by Mather et al. (1990) gave the absolute temperature of the CMBR of 2.735 ± 0.060 K, with a conservative systematic error estimate. The calibration process reported by Fixsen et al. (1994b) has enabled the

reduction of the error estimate to ± 0.010 K (95% CL systematic).

The calibration model includes an additive correction to the absolute temperature scale as a fixed adjustment made to the value read from the external calibrator thermometers. This parameter results in a determination of the color temperature scale, using the absolute frequency scale and the values of fundamental constants in the Planck law. The frequency scale was determined from the FIRAS observations of interstellar lines and is good to $\sim 0.03\%$ (95% CL). The average of the four low-frequency calibrations (two low-frequency detectors and the two dominant scan modes) gives an estimated adjustment of -7.4 ± 0.2 mK. The size of this shift is $\sim 0.3\%$, 10 times larger than the frequency scale uncertainty. The physical cause of such a temperature shift is under examination and may be as simple as a drift of the thermometer calibration in the 5 yr between test and launch. Eight additional thermometers from the same batch were tested 2 yr after launch and calibration shifts as high as 6 mK were seen at 2.7 K.

Until the physical cause for these discrepancies can be assigned, we adopt a best value for the temperature shift of half the value resulting from the photometric color temperature scale, or -4 mK, rounded to the nearest millikelvin. This gives equal weight to the direct thermometry and the photometry. We adopt an estimated total systematic temperature error of ± 0.010 K (95% CL systematic). This systematic uncertainty applies to comparisons between FIRAS derived temperatures and fluxes and those of other experiments, but not to comparisons of one frequency with another within the FIRAS data. Note that the 95% CL has been derived from a single degree of freedom, the width of a distribution of only two samples, and therefore is not a precise measure.

5. ANALYSIS OF SKY DATA

The analysis of the calibrated sky spectra to obtain the CMBR spectrum was done in four stages. First, a small temporally varying signal of unknown origin was detected, modeled, and removed. Second, a geometrical model of the Galaxy and dipole was applied to the entire data set to estimate their characteristic spectra. Third, the CMBR spectrum was determined as the average of the sky data taken during the last 6 weeks of operations, after subtracting the contribution from the Galaxy, dipole, and offset spectrum $c(\nu)$. Finally, the CMBR spectrum was compared to a blackbody spectrum and examined for possible deviations from that form.

5.1. *Model of Time Variation*

Multiple observations of many pixels on the sky, spaced up to 9 months apart, provide a sensitive test of instrument stability. As mentioned above, we detected a small temporally variable signal that has not been identified with any instrument component. The signal is also seen in the calibration data, indicating that its origin is within the instrument. In the 2–20 cm^{-1} range, this contaminating signal can be described by $u(\nu) \exp(-t/77.7)$, where t is the time of observation in days. This signal had a maximum amplitude of 2.9×10^{-8} ergs $\mathrm{cm}^{-2}\ \mathrm{s}^{-1}\ \mathrm{sr}^{-1}$ cm during the last 6 weeks of the mission.

After removal of the variable signal with the model described above, the rms scatter between multiple observations of the same pixel agrees with that expected from the intrinsic detector noise to within $\sim 5\%$. Detector noise was estimated from the dispersion in calibration interferograms taken over intervals of hours or less in conditions similar to those during sky observations.

The last 6 weeks of the mission produced the best data for measuring the CMBR spectrum. The temporal variation had decayed away, and the sky observations and calibrations were taken every week, with a $\sim 50\%$ duty cycle.

5.2. *Model of the Galaxy and Dipole*

The map of the FIRAS spectra shows three distinct components: a monopole (uniform) blackbody, a dipole variation in the temperature of this blackbody, and a high-frequency emission associated with the Galaxy. Fixsen et al. (1994a) do a more thorough dipole analysis using a different data selection than the present paper. Here we use the entire FIRAS data set to determine the spectra of these components. We model the data $S(\nu; l, b)$, where l, b are Galactic coordinates and ν is frequency, as follows:

$$S(\nu; l, b) = I_0(\nu) + D(l, b)d(\nu) + G(l, b)g(\nu) . \quad (2)$$

In this equation, the monopole is represented by the spectrum $I_0(\nu)$, the dipole variation is represented by the spatial distribution $D(l, b)$ and the spectrum $d(\nu)$, and the Galactic emission is represented by the spatial distribution $G(l, b)$ and the spectrum $g(\nu)$.

To make this separation the functions $D(l, b)$ for the dipole and $G(l, b)$ for the Galactic emission must be specified. The dipole is $D(l, b) = \cos(\theta)$, where θ is the angle between the observation and the maximum of the dipole. For the location of the dipole peak we used the determination of the *COBE* DMR (Smoot et al. 1992).

For $G(l, b)$ we used three different predictors, all of which gave essentially the same answer for the average Galactic spectrum $g(\nu)$ (Wright et al. 1994). The three models for $G(l, b)$ are (1) *COBE* DIRBE (Diffuse Infrared Background Experiment) 240 μm maps, convolved to FIRAS resolution; (2) the integrated power in the FIRAS high-frequency channel between 25 cm^{-1} and 65 cm^{-1}; and (3) a plane-parallel, $\csc(|b|)$ distribution.

In the present paper the DIRBE $G(l, b)$ is used. The whole FIRAS data set, corrected for the time-variable contamination source and excluding a box around the Galactic center ($|l| < 40°$, $|b| < 20°$), was fitted to derive $d(\nu)$ and $g(\nu)$. The effects of the Galactic modeling are discussed further in § 7 below.

5.3. *CMBR Spectrum Determination*

The sky data from the last 6 weeks of FIRAS operation, cut with the same box around the Galactic center, were used for the determination of the monopole by a weighted average over l and b:

$$I_0(\nu) = \langle S(\nu; l, b) - g(\nu)G(l, b) - d(\nu)D(l, b) - c(\nu) \rangle , \quad (3)$$

where $g(\nu)$ and $d(\nu)$ were from the all-sky fit and $c(\nu)$ was the photometric offset spectrum. The formal error in $I_0(\nu)$ is dominated by the contribution from detector noise.

6. FITTING MODELS TO THE COSMIC SPECTRUM

The monopole spectrum is well fitted by a Planck blackbody spectrum, and deviations are small, consistent with the earlier FIRAS results within their larger uncertainties (Mather et al. 1990; Shafer et al. 1992; and Cheng 1992). To determine or constrain any deviations from a blackbody, consider a generic cosmological model $S_c(\nu; p)$, where p is some cosmic parameter

quantifying the deviation from a blackbody, such as the Kompaneets y-parameter for Comptonized spectra or the dimensionless chemical potential μ for a Bose-Einstein photon distribution. Because the deviation is small, a linear fit

$$I_0(\nu) = B_\nu(T_0) + \Delta T \frac{\partial B_\nu}{\partial T} + G_0\, g(\nu) + p \frac{\partial S_c}{\partial p} \quad (4)$$

can be performed to the unknown parameters p, G_0, and ΔT. The first two terms are the Planck blackbody spectrum, with the temperature $T_0 + \Delta T$. The third term allows for a small additional Galactic contribution, with the same spectrum $g(\nu)$ derived from the all-sky data set, remaining in the monopole spectrum. The final term is the modeled deviation.

When p is fixed at 0, i.e., there is only a Galactic deviation fit, the maximum residual deviation is 3.4×10^{-8} ergs cm^{-2} s^{-1} sr^{-1} cm, which is 0.03% of the peak brightness of 1.2×10^{-4} ergs cm^{-2} s^{-1} sr^{-1} cm at 5.2 cm^{-1}. The weighted rms deviation in the frequency range 2–20 cm^{-1} is 0.01% of the peak brightness. The weighted rms is defined as $[\Sigma_i(\Delta_i^2/\sigma_i^2)/\Sigma_i(1/\sigma_i^2)]^{1/2}$, where Δ_i is the difference of the model and the data at spectrum point i, and σ_i is the uncertainty of the spectrum point i. The best-fit temperature is 2.726 K. When comparing this to values from other experiments, the systematic thermometry uncertainty of 0.010 K (95% CL systematic) should be included. The determination here gives the same mean temperature within the error as found by Fixsen et al. (1994a) from a slightly different data selection and method, because the random temperature errors caused by statistical effects are only 0.00001 K (95% CL), entirely negligible compared to the systematic error of the temperature scale calibration found by Fixsen et al. (1994b). Note also that the values and limits on any deviations p have no detectable dependence on the exact value of $T_0 + \Delta T$. The best-fit value of G_0 is equivalent to half the polar brightness of the Galaxy, suggesting that the high-latitude dust may be colder than the dust used to define $g(\nu)$.

There are two likely forms for distortions of the primeval spectrum produced during the plasma epoch before recombination, and we compute a limit independently for each. Energy release or conversion in the redshift range $10^5 < z < 3 \times 10^6$ produces a Bose-Einstein distribution, where the Planck law is modified by a dimensionless chemical potential μ (Zel'dovich & Sunyaev 1970):

$$S_\mu(\nu;\, T,\, \mu) = \frac{2hc^2\nu^3}{e^{x+\mu} - 1}, \quad (5)$$

where

$$x = hc\nu/kT \quad (6)$$

and ν is measured in cm^{-1}. The linearized deviation of S_μ from a blackbody is the derivative of equation (5) with respect to μ:

$$\frac{\partial S_\mu}{\partial \mu} = \frac{-T_0}{x} \frac{\partial B_\nu}{\partial T}. \quad (7)$$

The current FIRAS result is $\mu = (-12 \pm 11) \times 10^{-5}$, or 95% confidence level upper limit of $|\mu| < 3.3 \times 10^{-4}$. This result and those following are summarized in Table 1, including the effects of systematic uncertainties and the variation of the result according to the range of Galactic latitudes that are excluded from the fit.

Energy release at later times, $z < 10^5$, produces a Comptonized spectrum, a mixture of blackbodies at a range of temperatures. In the case of nonrelativistic electron temperatures this spectrum is described by the Kompaneets (1957) equation, parameterized by the value of y (Zel'dovich & Sunyaev 1969):

$$y = \int \frac{k(T_e - T_\gamma)}{m_e c^2}\, d\tau_e, \quad (8)$$

where T_e, T_γ, and τ_e are the electron temperature, the CMBR photon temperature, and the optical depth to electron Compton scattering. The distortion will be of the form (Zel'dovich & Sunyaev 1969)

$$\frac{\partial S_y}{\partial y} = T_0\left[\frac{x(1 + e^{-x})}{1 - e^{-x}} - 4\right]\frac{\partial B_\nu}{\partial T}. \quad (9)$$

The results are $y = (3 \pm 11) \times 10^{-6}$ with a 95% confidence level upper limit of 2.5×10^{-5}.

There are some obvious low-frequency systematic deviations in the residuals to the pure blackbody fit, and the high formal χ^2 per degree of freedom = 180/32 = 5.6 indicates a poor fit. The deviation at 10.76 cm^{-1} is not significant and is due to instrument vibration. Since this number was reported in preprint form, a factor of 1.35 has been shown to be the result of apodization, leaving a factor of 4 unexplained. However, pending further detailed study of possible instrument faults at these low frequencies, we cannot speculate on their nature. We emphasize that the size of the apparent deviations is greatest at those frequencies where diffractive effects, interferogram baseline curvature, and very low spectral resolving power and wide spectral sidebands cause the greatest difficulties in calibration (Fixsen et al. 1994b). We therefore conservatively increase the statistical errors by a factor, forcing the χ^2 to exactly equal 32, the number of degrees of freedom in the fit. The residuals, with the inflated errors, are shown in Figure 1 and listed in Table 2. The residuals can also be converted to an effective temperature of the CMBR as a function of frequency, which is shown in Figure 2 along with results from other measurements. A detailed comparison is given by Wright et al. (1994).

These limits for $|y|$ and $|\mu|$ are about 20–30 times smaller than those given in Mather et al. (1990). These new values place stringent constraints on theories of the early universe and the development of cosmic structure. As noted above, each constraint was derived from fitting only a single source of distortion at a time.

TABLE 1

ERRORS AND DEPENDENCE ON GALACTIC PLANE EXCLUSION ANGLE FROM 20° TO 40°

Parameter (unit)	Value	σ	Systemic Error	Galactic Range	95% CL
T_0 (K)	2.726	0.00001	0.005	±0.000012	0.010
$\mu(10^{-5})$	−12	8		−1 to −21	33
$y(10^{-6})$	3	8		−9 to +14	25

NOTE.—There is no known significant source of systematic error for y or μ besides the Galaxy. The quoted σ includes the effect of the simultaneous solution for a temperature shift and Galactic emission as well as y or μ.

7. GALACTIC CONTAMINATION

Our method for removing the Galactic spectrum assumes that the Galactic emission has the fixed spectral form $g(\nu)$ over the entire sky. The determination of $g(\nu)$ is dominated by Galactic plane emission, and there could be some variation from this form at higher latitudes. We vary the Galactic lati-

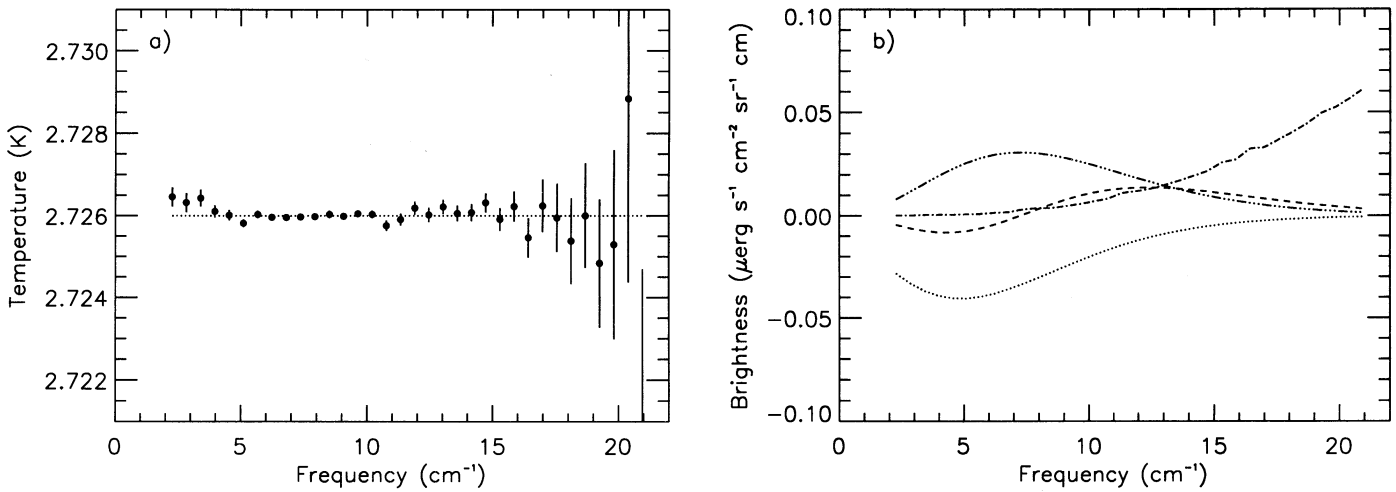

FIG. 1.—(*a*) FIRAS-measured CMBR residuals, $I_0 - B_\nu(T_0) - \Delta T(\partial B_\nu/\partial T) - G_0\, g(\nu)$. (*b*) Spectrum model components: the maximum allowed distortions (95% CL) $y = 2.5 \times 10^{-5}$ (*dashed line*) and $|\mu| = 3.3 \times 10^{-4}$ (*dotted line*); the Galaxy spectrum $g(\nu)$ scaled to one-fourth the flux at the Galactic pole (*dot-dashed line*), and the effects of a 200 μK temperature shift in T_0, $0.0002 \times [\partial B_\nu(T)/\partial T]$, (*dot-dot-dot-dashed line*).

tude cutoff used in deriving $I_0(\nu)$ in equation (3) to test the effect of variations in the Galactic spectrum from $g(\nu)$. Variations greater than the statistical uncertainty in any derived parameters, such as the cosmological term p, would most likely be due to an inadequacy in our Galactic model.

The central parameter values presented in this paper and in Wright et al. (1994) use the best-fit values where the cut was made at $|b|_{\rm min} = 30°$. As $|b|_{\rm min}$ was varied from 20° to 40°, the minimum and maximum best-fit values for the parameter p were noted, and we estimated the effective uncertainty due to the Galactic modeling process as $\sigma_g = (p_{\rm max} - p_{\rm min})/3$. This uncertainty was added in quadrature to the statistical parameter uncertainty ($\Delta\chi^2 = 1$, using the inflated error bars) to calculate the effective "1 σ" parameter uncertainty. This is a reasonable approach if one takes the measurements with different Galactic cut angles to be drawn from a uniform distribution with the measured width. In this case the deviation of a uniform distribution is the width divided by $12^{1/2}$, or about 3. While this is not a complete set of uncorrelated measurements, it is also informative of the actual uncertainty. The range of variation in μ due to the changes in the Galactic cut was $(-1$ to $-21) \times 10^{-5}$. The range of y values was $(-9$ to $+14) \times 10^{-6}$. Both ranges are included in the 95% confidence limits.

8. INTERPRETATION

The cosmological interpretation of the limits on y and μ are developed by Wright et al. (1994). We summarize their conclusions here briefly. Since the FIRAS spectrum with the Galactic dust emission removed is close to a blackbody, strict limits can be set on energy release after the big bang. For energy release during the Bose-Einstein period, the limit is $\Delta U/U = 0.71\ \mu$ where U is the energy of the cosmic background and ΔU is the energy converted from other forms. For energy release after

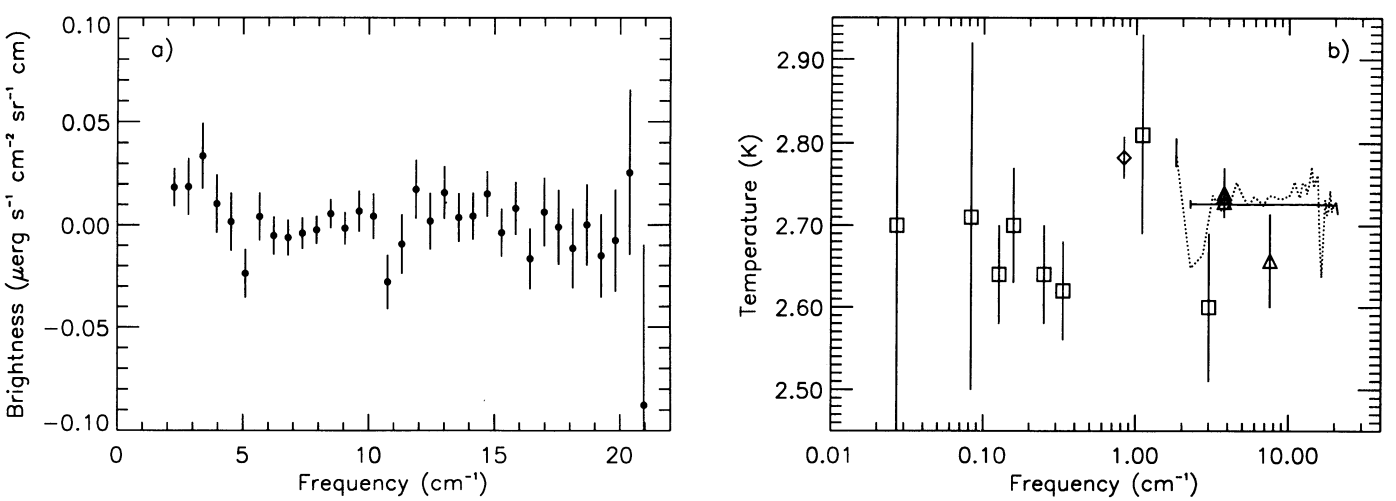

FIG. 2.—(*a*) FIRAS-measured temperature of CMBR vs. frequency. The systematic error in the temperature is 0.010 K (95% CL systematic). (*b*) FIRAS temperature (*straight line*) compared with previous measurements from the ground (*squares*) (Bensadoun et al. 1993; Bersanelli et al. 1989; De Amici et al. 1985, 1991; Kogut et al. 1990; Levin et al. 1992; Mandolesi et al. 1986; Sironi et al. 1990, 1991); balloon (*diamonds*) (Johnson & Wilkinson 1987), CN (*triangles*) (Kaiser 1990; Palazzi, Mandolesi, & Crane 1992; Roth 1992); and the COBRA rocket spectrometer (*dotted line*) (Gush, Halpern, & Wishnow 1990). The size of the COBRA and FIRAS 1 σ systematic temperature errors is shown by the vertical bars at the beginning of their spectra.

TABLE 2

RESIDUAL OF MONOPOLE SPECTRUM

Frequency (cm^{-1})	Residual	Error (1 σ)	Galaxy at Pole
2.27	18	9	1
2.83	19	14	1
3.40	34	16	2
3.96	10	14	2
4.53	2	14	2
5.10	−24	12	4
5.66	4	12	4
6.23	−5	9	7
6.80	−6	9	9
7.36	−4	8	15
7.93	−2	7	18
8.49	6	7	18
9.06	−2	8	23
9.63	7	10	28
10.19	4	11	35
10.76	−28	13	42
11.33	−9	15	55
11.89	17	14	59
12.46	2	14	65
13.03	16	13	74
13.59	4	12	85
14.16	4	11	97
14.72	15	11	108
15.29	−4	12	129
15.86	8	13	136
16.42	17	15	163
16.99	6	17	166
17.56	−1	18	184
18.12	−12	19	202
18.69	0	20	222
19.26	−15	20	247
19.82	−8	25	261
20.39	25	40	282
20.95	−88	78	306

NOTE.—Intensities in 10^{-9} ergs cm^{-2} s^{-1} sr^{-1} cm.

that but before decoupling, the limit is $\Delta U/U = 4$ y. After decoupling, the density of any uniform diffuse intergalactic medium hot enough to produce the observed diffuse X-ray background is two orders of magnitude too small to produce that background. Limits on subtraction of the Galactic dust emission show that other dusty galaxies and Population III star bursts can be limited to converting $\leq 1\%$ of the cosmic baryon abundance from H to He for $z < 80$. The steady state theory is conclusively ruled out, since the optical depth of dust necessary to thermalize the cosmic background radiation to the degree shown by FIRAS would entirely prevent the observation of distant galaxies and quasars at millimeter wavelengths.

9. SUMMARY AND CONCLUSIONS

The FIRAS spectrum of the cosmic microwave background radiation agrees with a blackbody spectrum to high accuracy. The CMBR spectrum is the result of fitting a model including a dipole and a dust map derived from 240 μm data, excluding a region around the Galactic center. The fitted temperature is 2.726 ± 0.010 K (95% CL systematic), where the error is dominated by our estimate of the thermometry errors. The maximum deviation from the fit is 3.4×10^{-8} ergs cm^{-2} s^{-1} sr^{-1} cm, only 0.03% of the peak brightness, and the 2–20 cm^{-1} weighted rms errors is only 0.01% of the peak. The corresponding limit on $|y|$ is 2.5×10^{-5} and the limit on $|\mu|$ is 3.3×10^{-4} (95% CL).

We thank the NASA/GSFC technical staff, especially M. Roberto and R. Maichle, for their thoughtful and original approaches to solving problems in this instrument, both before and after launch. There were many difficulties in extending the accuracy of far-infrared spectrophotometers by two orders of magnitude, particularly with a moving cryogenic interferometrically precise mirror mechanism required to operate without attention after a rocket launch. We also thank the computer scientists and analysists who operated the *COBE*, processed the data, and solved problems in software that could no longer be solved with hardware. In particular, we thank S. Alexander, W. Barnes, D. Bazell, J. Gales, N. Gonzales, S. Macwan, D. Pfenning, F. Shuman, A. Trenholme, H. Wang, D. Wynne, and W. Young.

REFERENCES

Bennett, C. L., et al. 1992, ApJ, 396, L7
———. 1993, in The Evolution of Galaxies and Their Environment, ed. H. A. Thronson & J. M. Shull (Dordrecht: Kluwer), in press
Bensadoun, M., Bersanelli, M., De Amici, G., Kogut, A., Levin, S. M., Limon, M., Smoot, G. F., & Witebsky, C. 1993, ApJ, 409, 1
Bersanelli, M., Witebsky, C., Bensadoun, M., De Amici, G., Kogut, A., Levin, S., & Smoot, G. 1989, ApJ, 339, 632
Boggess, N. W., et al. 1992, ApJ, 397, 420
Cheng, E. S. 1992, in Proc. International Symposium on Observational Cosmology, Milan, Italy, September 1992, in press
De Amici, G., et al. 1991, ApJ, 381, 341
———. 1985, ApJ, 298, 710
Dicke, R. H., Peebles, P. J. E., Roll, P. G., & Wilkinson, D. T. 1965, ApJ, 142, 414
Fixsen, D. J., et al. 1994a, ApJ, 420, 445
Fixsen, D. J., et al. 1994b, ApJ, 420, 457
Gush, H. P., Halpern, M., & Wishnow, E. H. 1990, Phys. Rev. Lett., 65, 537
Johnson, D. G., & Wilkinson, D. T. 1987, ApJ, 313, L1
Kaiser, M. E. 1990, Ph.D. thesis, UCLA
Kogut, A., Bensadoun, M., de Amici, G., Levin, S., Smoot, G. F., & Witebsky, C. 1989, ApJ, 355, 102
Kogut, A. 1993, in Topics on Astrofundamental Physics, ed. N. Sanchez & A. Zichichi (London: World Scientific), 213
Kompaneets, A. S. 1957, JETP, 4, 730
Levin, S., Bensadoun, M., Bersanelli, M., De Amici, G., Kogut, A., Limon, G., & Smoot, G. F. 1992, ApJ, 396, 3
Mather, J. C., et al. 1990, ApJ, 354, L37
Mandolesi, N., et al. 1986, ApJ, 310, 561
Palazzi, E., Mandolesi, N., & Crane, P. 1992, ApJ, 398, 53
Peebles, P. J. E. 1971, Physical Cosmology (Princeton: Princeton Univ. Press)
Penzias, A. A., & Wilson, R. W. 1965, ApJ, 142, 419
Roth, K. C. 1992, Ph.D. thesis, Northwestern Univ.
Shafer, R. A., et al. 1992, BAAS, 23, 1398
Sironi, G., Bonelli, G., & Limon, M. 1991, ApJ, 378, 550
Sironi, G., Limon, M., Marcelline, G., Bonelli, G., Bersanelli, M., Conti, G., & Reif, K. 1990, ApJ, 357, 301
Sunyaev, R. A., & Zel'dovich, Ya. B. 1980, ARA&A, 18, 537
Smoot, G. F., et al. 1992, ApJ, 396, L1
Thaddeus, P. 1972, ARA&A, 10, 305
Weiss, R. 1980, ARA&A, 18, 489
Wright, E. L., et al. 1991, ApJ, 381, 200
Wright, E. L., et al. 1994, ApJ, 420, 450
Zel'dovich, Ya. B., & Sunyaev, R. A. 1969, Ap&SS, 4, 301
———. 1970, Ap&SS, 7, 20